

LETTER TO THE EDITOR

The super-orbital modulation of supergiant high-mass X-ray binaries

E. Bozzo¹, L. Oskinova^{2,3}, A. Lobel⁴, and W.-R. Hamann²

¹ Department of Astronomy, University of Geneva, Chemin d'Ecogia 16, 1290 Versoix, Switzerland
e-mail: enrico.bozzo@unige.ch

² Institut für Physik und Astronomie, Universität Potsdam, Karl-Liebknecht-Strasse 24/25, 14476 Potsdam, Germany

³ Kazan Federal University, Kremlevskaya Str., 18, Kazan 420008, Russia

⁴ Royal Observatory of Belgium, Ringlaan 3, 1180 Brussels, Belgium

Received 11 September 2017 / Accepted 4 October 2017

ABSTRACT

The long-term X-ray light curves of classical supergiant X-ray binaries and supergiant fast X-ray transients show relatively similar super-orbital modulations, which are still lacking a sound interpretation. We propose that these modulations are related to the presence of corotating interaction regions (CIRs) known to thread the winds of OB supergiants. To test this hypothesis, we couple the outcomes of three-dimensional (3D) hydrodynamic models for the formation of CIRs in stellar winds with a simplified recipe for the accretion onto a neutron star. The results show that the synthetic X-ray light curves are indeed modulated by the presence of the CIRs. The exact period and amplitude of these modulations depend on a number of parameters governing the hydrodynamic wind models and on the binary orbital configuration. To compare our model predictions with the observations, we apply the 3D wind structure previously shown to well explain the appearance of discrete absorption components in the UV time series of a prototypical B0.5I-type supergiant. Using the orbital parameters of IGR J16493-4348, which has the same B0.5I donor spectral type, the period and modulations in the simulated X-ray light curve are similar to the observed ones, thus providing support to our scenario. We propose that the presence of CIRs in donor star winds should be considered in future theoretical and simulation efforts of wind-fed X-ray binaries.

Key words. X-rays: stars – X-rays: binaries – gamma rays: stars – stars: massive – stars: neutron

1. Introduction

Supergiant high-mass X-ray binaries (SgXBs) are a sub-class of high-mass X-ray binaries (HMXBs) hosting a compact object and an OB supergiant star (see [Walter et al. 2015](#), for a recent review). Two groups are typically distinguished; the classical systems, which show a virtually persistent high X-ray luminosity, and the supergiant fast X-ray transients (SFXTs), which feature a still highly debated and peculiarly prominent variability in X-rays ([Martínez-Núñez et al. 2017](#)). The bulk of the X-ray radiation from the SgXBs can be reasonably well explained as being due to the accretion of the stellar wind from the OB supergiant onto a highly magnetized neutron star (NS), with no evidence supporting the presence of long-lived accretion disks ([Bozzo et al. 2008](#); [Shakura et al. 2012](#); [Romano et al. 2015](#); [Hu et al. 2017](#)). No clear indication has yet been reported of systematic differences between the properties of the supergiant stellar winds in classical systems and SFXTs (Hainich et al., in prep.), which also share similar orbital periods ([Lutovinov et al. 2013](#); [Bozzo et al. 2015](#)) and super-orbital modulations (see [Table 1](#) and [Corbet & Krimm 2013](#)).

The super-orbital variability in disk-accreting X-ray binaries is usually ascribed to the precession of the disk or to the precession of the compact object in its center (see, e.g., the cases of Her X-1, SMC X-1, and LMC X4; [Petterson 1975](#); [Ogilvie & Dubus 2001](#); [Postnov et al. 2013](#)), but a solid interpretation of the same phenomenon in wind-fed binaries is still lacking. The light curves of the latter folded on their super-orbital period display a large variety of morphologies and modulations

Table 1. SgXBs with confirmed orbital (P_{NS}) and super-orbital (P_{SO}) periods from [Corbet & Krimm \(2013\)](#).

Source name	Class	P_{NS} (days)	P_{SO} (days)
IGR J16479-4514	SFXT	3.3199 ± 0.0005	11.880 ± 0.002
IGR J16418-4532	SgXB	3.7389 ± 0.0001	14.730 ± 0.006
4U 1909+07	SFXT	4.4003 ± 0.0004	15.180 ± 0.003
IGR J16493-4348	SgXB	6.782 ± 0.001	20.07 ± 0.01
2S 0114+650	SgXB	11.591 ± 0.003	30.76 ± 0.03

that are stable over years, although the sources are generally thought to be accreting from a much less regularly structured environment compared to that provided by an accretion disk. In the case of the classical SgXB 2S 0114+650, [Farrell et al. \(2008\)](#) reported the detection of spectral slope changes as a function of the super-orbital phase but could not detect corresponding variations in the absorption column density (also due to the limited coverage at energies $\lesssim 3$ keV provided by the instruments onboard RXTE; [Bradt et al. 1993](#)). These authors suggested that the most likely cause of the super-orbital variability was a modulation of the mass-loss rate from the supergiant star. For all other systems showing a super-orbital modulation, the only X-ray data providing coverage on different super-orbital phases are those collected with *Swift*/BAT ([Gehrels et al. 2004](#); [Barthelmy et al. 2005](#)). The relatively low signal-to-noise ratio of these data and

the energy band-pass limited to ≥ 15 keV have hampered so far any investigation of spectral variability as a function of the super-orbital phase. [Koenigsberger et al. \(2006\)](#) proposed that the mass-accretion-rate modulation could be produced as a consequence of tidal interaction-driven oscillations of the supergiant star, but the authors showed that such a mechanism only works for strictly circular orbits. [Corbet & Krimm \(2013\)](#) also discussed the possibility that the super-orbital modulations are due to a third body orbiting the inner massive binary. However, the same authors highlighted that a stable three-body solution requires a hierarchical system with the third body in a very distant orbit, while all super-orbital modulations discovered so far in SgXBs are not longer than roughly three times the orbital periods of these sources.

We propose here that the super-orbital periodicities in classical SgXBs and SFXTs are produced as a consequence of the interaction between the compact object with the so-called “corotating interaction regions” threading the winds of OB supergiants.

2. Corotating interaction regions around OB supergiants

The stellar winds of OB supergiants are well known to be characterized by complex velocity and density structures (see, e.g., [Puls et al. 2008](#), and references therein). The smaller structures, referred to as “clumps”, are typically endowed with an increased density of a factor of ≥ 10 compared to a smooth wind and can be as large as $\sim 0.1 R_*$, where R_* is the OB supergiant radius. Clumps are usually invoked to interpret the stochastic X-ray variability displayed by SgXBs on time scales of 10–1000 s (see, e.g., [Martínez-Núñez et al. 2017](#), and references therein).

The existence of larger structures in the OB supergiant winds was suggested in the early 80s ([Mullan 1984](#)), and confirmed by the detection of discrete absorption components (DACs; see, e.g., [Underhill 1975](#)). These features are observed to propagate blue-ward on time-scales comparable with the stellar rotation through the profiles of UV resonance lines in OB supergiants ([Massa et al. 1995a](#); [Prinja & Crowther 1998](#)). [Cranmer & Owocki \(1996\)](#) used hydrodynamic models to show that irregularities on the stellar surface, related either to dark/bright spots, magnetic loops, or non-radial pulsations, can lead to the formation of corotating interaction regions (CIRs) causing spiral-shaped density and velocity perturbations in the stellar wind up to several tens of stellar radii. The CIRs are invoked to explain modulations of the X-ray emission observed in single OB stars ([Oskinova et al. 2001](#); [Nazé et al. 2013](#); [Massa et al. 2014](#)).

An advanced model to reproduce the observational properties of DACs in OB supergiants with CIRs was developed by [Lobel & Blomme \(2008\)](#), who also investigated the dependence of the extension, velocity, and density profile variations of these structures as a function of the different properties of the stellar surface spots from which they originate. The intensity of the spot, its size, and its rotational velocity (that could in principle be different from that of the star) are the main parameters regulating the density/velocity contrast of the CIR compared to the surrounding unperturbed stellar wind, typically limited to a factor of a few. A larger rotational velocity of the spot also increases the winding of the spiral arms. The available observations of the UV variability of massive-star resonance lines can be used to constrain all the spot free parameters of the model.

We show in [Fig. 1](#) a hydrodynamic simulation of [Lobel & Blomme \(2008\)](#) obtained from the application of the

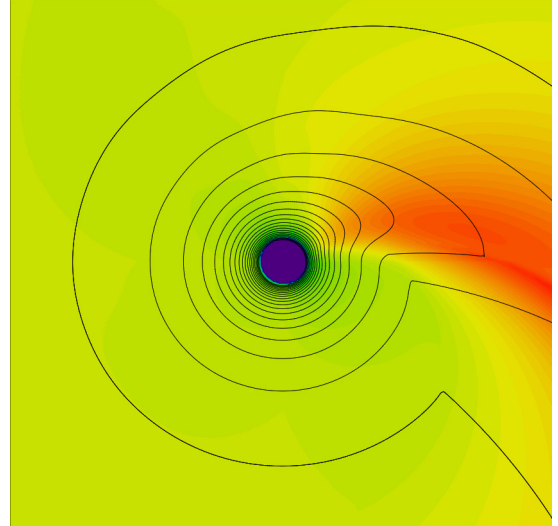


Fig. 1. An example of hydrodynamic calculations of the CIR in the wind of the B0.5 Ib supergiant J Pup. There is a bright spot on the stellar surface producing a single CIR. The spot is assumed to be 20% brighter than the stellar surface, and is characterized by an angular diameter of 20° . A full revolution of the CIR occurs in ~ 10.3 days. The colors code the wind density of the CIR model relative to the density of the unperturbed, smooth wind. The maximum over-density in the CIR is by a factor 1.22 (red colors). In wind regions shown in yellow this ratio hardly deviates from unity, while in the green regions the wind is rarified by a factor lower than 0.97. The black solid drawn lines show 20 overplotted contours of equal radial velocity in the hydrodynamic rotating wind model. The outermost curve marks the isovelocity line at an outflow velocity of 1460 km s^{-1} , while the curves at smaller distances from the stellar surface are shown for decreasing steps of 73 km s^{-1} . The case with two CIRs mentioned later in this paper is produced by assuming an additional spot that is 8% brighter than the surface of the supergiant star and has an angular diameter of 30° .

Zeus-3D code for a radiatively driven rotating wind in the B0.5 Ib supergiant J Pup (HD 64760). This star has a mass of $20 M_\odot$, a radius of $22 R_\odot$, a mass-loss rate of $9 \times 10^{-7} M_\odot \text{ yr}^{-1}$, and a terminal wind velocity of 1500 km s^{-1} (see [Table 1 of Lobel & Blomme 2008](#)).

3. The CIR-induced super-orbital modulation in SgXBs

In order to show how the presence of CIRs around the supergiant star can introduce a super-orbital modulation of the X-ray luminosity from a SgXB, we assume here a simplified NS accretion scenario, following the treatment in [Oskinova et al. \(2012\)](#). The cross section of the NS for the capture of the stellar wind material is provided by the so-called accretion radius, $r_{\text{accr}} = \frac{2Gm_X}{v_{\text{rel}}^2}$, where m_X is the NS mass and v_{rel} is the relative velocity between the NS and the massive star wind. For the CIR, both the radial and tangential components of the velocity at the NS location are taken into account in the computation. The mass accretion rate onto the NS is given by $S_{\text{accr}} = 4\pi\zeta \frac{(Gm_X)^2}{v_{\text{rel}}^3} \rho$, and the correspondingly released X-ray luminosity is $L_X^{\text{d}} = \eta S_{\text{accr}} c^2$. In the equations above, we indicated with c the speed of light, with ρ the local wind density (derived from the outputs of the hydrodynamic model), and considered for all cases of interest $\zeta \sim 1$ and $\eta \sim 0.1$ (ζ is a parameter included to take into account corrections related to the contribution of the radiation pressure and the finite cooling time of the gas, while η parametrizes the efficiency

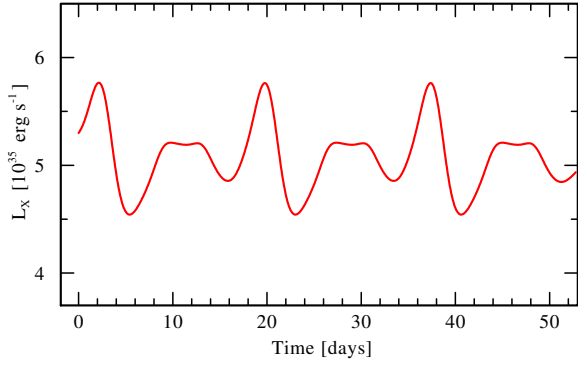


Fig. 2. Simulated long-term light curve of IGR J16493-4348, assuming a single CIR in this system rotating with a period of ~ 10.3 days.

of accretion onto a NS; see, e.g., Davidson & Ostriker 1973). It is clear from this simplified treatment that both the density and velocity contrasts of the CIR compared to the smooth wind can affect the resulting X-ray luminosity, as they can significantly alter the mass-accretion rate and the size of the NS cross section for the capture of the wind material.

Let's consider first a case in which the NS orbital period is given by P_{NS} and a single CIR rotating with a period P_{CIR} is present in the wind of the supergiant companion. A difference between P_{NS} and P_{CIR} can be expected in a not-synchronously rotating binary (see, e.g., Koenigsberger et al. 2006, and references therein), or in case the stellar spot does not rotate with the same velocity of the supergiant star (Lobel & Blomme 2008). The mass-accretion rate onto the NS is altered every time the compact object encounters the CIR along its orbit and the amplitude of the variation is regulated by the CIR velocity/density contrast compared to the rest of the stellar wind. The period of the super-orbital modulation, P_{SO} , is thus given by the difference between the NS and the CIR angular velocities:

$$P_{\text{SO}} = \frac{1}{\left| \frac{1}{P_{\text{NS}}} - \frac{1}{P_{\text{CIR}}} \right|} = \left| \frac{P_{\text{NS}} P_{\text{CIR}}}{P_{\text{CIR}} - P_{\text{NS}}} \right|. \quad (1)$$

As an example, we consider in detail the case of the classical SgXB, IGR J16493-4348. The donor star in this system has the same spectral type as JPup and the estimated distance is 6–26 kpc (see Martínez-Núñez et al. 2017, and references therein). Given the typical parameters of a B0.5 Ib star (Sect. 2) and the measured orbital period of the NS in IGR J16493-4348 (Table 1), the separation between the compact object and the supergiant is $\sim 1.8 R_*$. According to Eq. (1), a single CIR rotating with a period of ~ 10.3 days is thus expected to give rise to a super-orbital period of ~ 20 days, as indeed observed in this source. The X-ray light curve simulated using the output of the hydrodynamic model for the CIR in JPup (Fig. 2) is characterized by an average luminosity which is in good agreement with the observations of IGR J16493-4348¹. The amplitude of the modulation is smaller than that observed from IGR J16493-4348, but the exact value depends on, for example, the brightness of the spot on the stellar surface responsible for the CIR generation (in the present case the hydrodynamical simulations were tuned to reproduce the results of UV spectroscopic monitoring for JPup).

In a situation in which multiple CIRs are present and intercept the plane of the NS orbit, it would be naturally expected that

¹ The absolute value of the average X-ray luminosity from IGR J16493-4348 ranges from $\sim 10^{35}$ erg s⁻¹ to $\sim 10^{36}$ erg s⁻¹, depending on the poorly known distance to the source (6–26 kpc).

their density/velocity contrasts are significantly different, reflecting the distinct properties of the stellar surface spots from which they originated. Assuming that n CIRs cross the NS orbit, the overall period of the super-orbital modulation will be in this case $n \times P_{\text{SO}}$. Several peaks of variable intensities can thus originate in the modulation profile depending on the different CIR density/velocity contrast at the NS location. We show in the bottom plot of Fig. 3 an example in which a second CIR is included in our calculations, giving rise to a double-peaked super-orbital modulation (see also the caption of Fig. 1). A multiple-peaked super-orbital modulation seems particularly interesting to reproduce structured profiles of the folded X-ray light curves displayed by, for example, the classical SgXB 4U 1909+07 and the SFXT IGR J16479-4514 (see Figs. 8 and 10 of Corbet & Krimm 2013). Figure 3 shows that the super-orbital variability critically depends on the difference between P_{NS} and P_{CIR} . Although CIRs seem to be a ubiquitous property of all supergiant stars (see, e.g., Massa & Prinja 2015, and references therein), the detectability of a super-orbital modulation in the currently proposed model could be hampered in all those unfavorable cases where $P_{\text{NS}} \simeq P_{\text{CIR}}$ and P_{SO} exceeds the available observational time-span for a SgXB.

Although all the free parameters on the number and properties of the CIRs can be fine tuned to obtain a reasonable match with the properties of the super-orbital modulations of all sources in Table 1, there is not an obvious way to explain the empirical relation connecting the system orbital and super-orbital period as shown by Corbet & Krimm (2013; see their Fig. 1). If the relation is confirmed by future observations, a better understanding of the CIR formation in the SgXBs will be required to investigate the possibility of explaining this observational finding in the current model.

We neglected in the present simplified approach the role of the NS spin period and magnetic field, as well as the effect of eccentric orbits and the interaction between the X-rays from the NS and the stellar wind. A strong NS magnetic field and slow spin period can induce large modulations of the X-ray luminosity, due to the onset of magnetic and/or centrifugal gates (Grebenev & Sunyaev 2007; Bozzo et al. 2008). While this is relevant to explain the short time-scale X-ray variability (~ 10 – 1000 s) displayed by classical SgXBs and SFXTs (Bozzo et al. 2016), we expect this variability to be largely smoothed out when considering the much longer integration times corresponding to the super-orbital modulations (tens of days).

As described in Bozzo et al. (2016), the lack of a proper treatment of the X-ray illumination of the stellar wind by the accreting compact object limits the validity of the outcomes of the calculations to low-luminosity SgXBs ($L_X \lesssim 10^{35}$ erg s⁻¹) and can only provide indications in the cases of brighter systems. This effect is thus unlikely to be critical in the case of the SFXTs, as their average X-ray luminosity is generally far below the critical level required to produce a systematic disruption of the stellar wind on scales that are as large as those expected for the CIRs (see, e.g., Ducci et al. 2010, and references therein). However, this might not apply to bright persistent classical wind-fed SgXBs with average X-ray luminosities $\gg 10^{36}$ – 10^{37} erg s⁻¹ (e.g., Vela X-1; Watanabe et al. 2006; Sander et al. 2017), which we predict to not display super-orbital modulations. We note that all SgXBs discovered so far to display a super-orbital modulation are characterized by relatively low long-term luminosities, the brightest being IGR J16493-4348 with an estimated average X-ray luminosity of $\sim 1.5 \times 10^{36}$ erg s⁻¹ when the largest allowed distance of 26 kpc is considered.

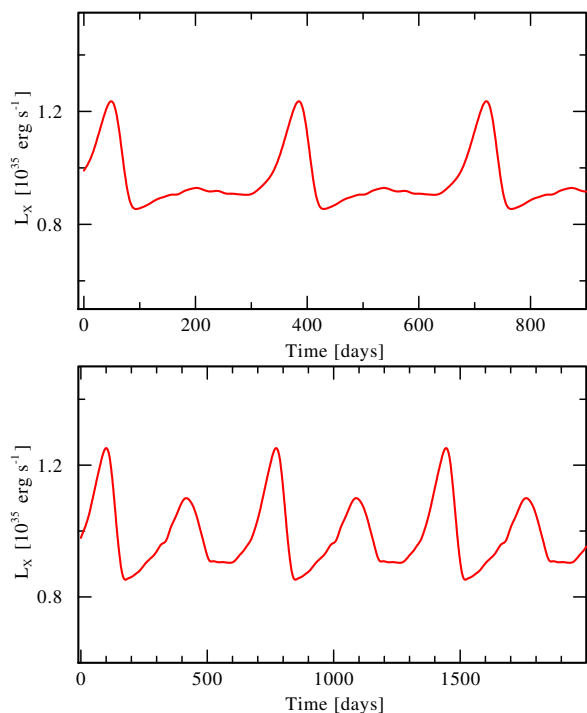


Fig. 3. *Top:* same as Fig. 2 but assuming an orbital separation of $2.5 R_*$, corresponding to an orbital period of ~ 10.6 days. As this is only slightly larger than the CIR period (~ 10.3 days), the super-orbital modulation occurs on a much longer time-scale (~ 330 days). *Bottom:* same as above but using two CIRs. The super-orbital modulation is now characterized by a double asymmetric peak repeating every ~ 660 days, corresponding to the fact that the NS is crossing two CIRs with different density/velocity contrasts along its orbit.

Finally, circular orbits were used in our calculation to limit the number of required hydrodynamic runs and to provide more intuitive examples to promote the proposed scenario. However, we do not expect that our conclusions would change significantly with the introduction of a relatively small eccentricity ($\lesssim 0.2$; Corbet & Krimm 2013, and references therein), as the range of orbital separations spanned by the NSs would be limited and the density/velocity contrasts within each CIR are expected to undergo major variations only on several stellar radii (for reasonable assumptions of the model parameters).

4. Discussion and conclusions

We propose in this Letter that the still poorly understood super-orbital variability displayed by several classical SgXBs and SFXTs is related to the presence of CIRs in the winds of their OB supergiants. The mechanisms leading to the formation of CIRs are not yet fully understood and the model considered in Sect. 2 exploits the most widely accepted idea that CIRs are driven by spots on the supergiant surface with a number of free parameters that can be adjusted to reproduce the observational properties of DACs in many isolated OB supergiants. At present, no observations of DACs are available for the donor stars in classical SgXBs and SFXTs, and it is thus difficult to present an exhaustive exploration of the entire model parameter space (this is beyond the scope of this work, given also the computationally expensive runs of the hydrodynamic simulations). However, the examples provided in Sect. 3 show that the number and physical characteristics of the CIRs can be adjusted within reasonable boundaries to reproduce the main observed properties of the super-orbital modulations displayed by all sources in Table 1.

This paves the way to future theoretical and simulation efforts exploring the proposed model in more detail and overcoming the simplifications adopted in the current approach, including the presence of the X-ray irradiation of the stellar wind and eccentric orbits.

We remark that an important open question in the context of the present interpretation of the super-orbital modulations is whether or not CIRs can be stable for years. Indeed, most of the DAC observations leading to the concept of CIRs were carried out as part of the MEGA campaign (Massa et al. 1995b) performed with the IUE satellite (Boggess et al. 1978) and were not repeated afterwards. Long dedicated monitoring campaigns of the UV spectroscopic variability of the previously observed supergiant stars and the other supergiants hosted in the SgXBs are thus critically required.

Acknowledgements. We thank the anonymous referee for constructive comments, which helped to improve the paper. This publication was motivated by a team sponsored by the ISSI in Bern, Switzerland. E.B. and L.O. thank ISSI for the financial support during their stay in Bern. E.B. is grateful for the hospitality of the Institut für Physik und Astronomie (Universität Potsdam) during part of this work. E.B. acknowledges a financial contribution for travel from the Swiss Society for Astronomy and Astrophysics. L.O. acknowledges support by the DLR grant 50 OR 1302 and partial support by the Russian Government Program of Competitive Growth of Kazan Federal University. A.L. acknowledges partial financial support from the Belgian Federal Science policy Office under contract No. BR/143/A2/BRASS and by the ESA-Gaia Prodex Programme 2015–2017.

References

- Barthelmy, S. D., Barbier, L. M., Cummings, J. R., et al. 2005, *Space Sci. Rev.*, **120**, 143
- Boggess, A., Carr, F. A., Evans, D. C., et al. 1978, *Nature*, **275**, 372
- Bozzo, E., Falanga, M., & Stella, L. 2008, *ApJ*, **683**, 1031
- Bozzo, E., Romano, P., Ducci, L., Bernardini, F., & Falanga, M. 2015, *Adv. Space Res.*, **55**, 1255
- Bozzo, E., Oskinova, L., Feldmeier, A., & Falanga, M. 2016, *A&A*, **589**, A102
- Bradt, H. V., Rothschild, R. E., & Swank, J. H. 1993, *A&AS*, **97**, 355
- Corbet, R. H. D., & Krimm, H. A. 2013, *ApJ*, **778**, 45
- Cranmer, S. R., & Owocki, S. P. 1996, *ApJ*, **462**, 469
- Davidson, K., & Ostriker, J. P. 1973, *ApJ*, **179**, 585
- Ducci, L., Sidoli, L., & Paizis, A. 2010, *MNRAS*, **408**, 1540
- Farrell, S. A., Sood, R. K., O'Neill, P. M., & Dieters, S. 2008, *MNRAS*, **389**, 608
- Gehrels, N., Chincarini, G., Giommi, P., et al. 2004, *ApJ*, **611**, 1005
- Grebenev, S. A., & Sunyaev, R. A. 2007, *Astron. Lett.*, **33**, 149
- Hu, C.-P., Chou, Y., Ng, C.-Y., Lin, L. C.-C., & Yen, D. C.-C. 2017, *ApJ*, **844**, 16
- Koenigsberger, G., Georgiev, L., Moreno, E., et al. 2006, *A&A*, **458**, 513
- Lobel, A., & Blomme, R. 2008, *ApJ*, **678**, 408
- Lutovinov, A. A., Revnivtsev, M. G., Tsygankov, S. S., & Krivonos, R. A. 2013, *MNRAS*, **431**, 327
- Martínez-Núñez, S., Kretschmar, P., Bozzo, E., et al. 2017, *Space Sci. Rev.*, in press, DOI: 10.1007/s11214-017-0340-1
- Massa, D., Prinja, R. K., & Fullerton, A. W. 1995a, *ApJ*, **452**, 842
- Massa, D., Fullerton, A. W., Nichols, J. S., et al. 1995b, *ApJ*, **452**, L53
- Massa, D., Oskinova, L., Fullerton, A. W., et al. 2014, *MNRAS*, **441**, 2173
- Massa, D., & Prinja, R. K. 2015, *ApJ*, **809**, 12
- Mullan, D. J. 1984, *ApJ*, **283**, 303
- Nazé, Y., Oskinova, L. M., & Gosset, E. 2013, *ApJ*, **763**, 143
- Ogilvie, G. I., & Dubus, G. 2001, *MNRAS*, **320**, 485
- Oskinova, L. M., Clarke, D., & Pollock, A. M. T. 2001, *A&A*, **378**, L21
- Oskinova, L. M., Feldmeier, A., & Kretschmar, P. 2012, *MNRAS*, **421**, 2820
- Peterson, J. A. 1975, *ApJ*, **201**, L61
- Postnov, K., Shakura, N., Staubert, R., et al. 2013, *MNRAS*, **435**, 1147
- Prinja, R. K., & Crowther, P. A. 1998, *MNRAS*, **300**, 828
- Puls, J., Vink, J. S., & Najarro, F. 2008, *A&ARv*, **16**, 209
- Romano, P., Bozzo, E., Mangano, V., et al. 2015, *A&A*, **576**, L4
- Sander, A. A. C., Fürst, F., Kretschmar, P., et al. 2017, *A&A*, submitted [arXiv:1708.02947]
- Shakura, N., Postnov, K., Kochetkova, A., & Hjalmarsdotter, L. 2012, *MNRAS*, **420**, 216
- Underhill, A. B. 1975, *ApJ*, **199**, 691
- Walter, R., Lutovinov, A. A., Bozzo, E., & Tsygankov, S. S. 2015, *A&ARv*, **23**, 2
- Watanabe, S., Sako, M., Ishida, M., et al. 2006, *ApJ*, **651**, 421